JOC The Journal of Organic Chemistry

pubs.acs.org/joc Article

Photoinduced Skeletal Rearrangement of *N*-Substituted Colchicine Derivatives

Dominika Czerwonka, Szymon Sobczak, Tomasz Pędziński, Ewa Maj, Joanna Wietrzyk, Lech Celewicz, Andrzej Katrusiak, and Adam Huczyński*

Cite This: *J. Org. Chem.* 2021, 86, 11029–11039

Read Online

ACCESS | Metrics & More | Article Recommendations | Supporting Information

ABSTRACT: Colchicine is an active pharmaceutical ingredient widely used for treating gout, pericarditis, and familial Mediterranean fever with high antimitotic activity. The photoisomerization of colchicine deactivates its anti-inflammatory and antimitotic properties. However, despite numerous reports on colchicine derivatives, their photostability has not been investigated in detail. This report reveals the effects of UV-induced rearrangement on the structure and reports the biological activity of new *N*-substituted colchicine derivatives.

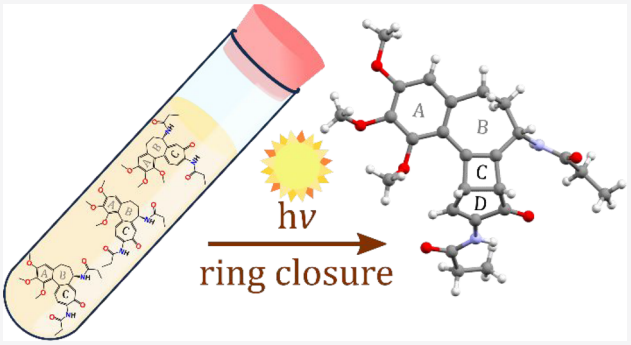

Many organic compounds, including drugs, exhibit low photostability. Some compounds decompose upon exposition to light in minutes, while it takes weeks or months for others. The ultraviolet component of sunlight or of artificial light affects the chemical structure of compounds and the physicochemical properties of the products, such as their color, solubility, or viscosity.[1] Most importantly, the photodecomposed drugs lose therapeutic activity and can cause severe side effects.[2] Transparent plastic packages or amber and brown glass vials offer only a little protection from UV radiation in the case of some highly photolabile compounds.[3] The photodegradation often limits the application or eveneliminates highly active drugs, so photostability has become an important parameter in drug characterization.

Colchicine (Figure 1), a pseudoalkaloid produced by *Colchicum autumnale*, is used as the first-line therapy for gout, pericarditis, and familial Mediterranean fever.[4−7] Colchicine is also known for its high capability of binding to the tubulin in rapidly dividing cancer cells, which inhibits microtubule polymerization leading to mitosis arrest and finally to cell apoptosis.[8−10] However, the severe toxicity and photosensitivity limit the applications of this compound,[11−13] although its numerous new derivatives are reported each year.[12−27] When colchicine is exposed to sunlight, it transforms to a mixture of α-, β-, and γ-lumicolchicine, where β- and γ-lumicolchicine are stereoisomers and α-lumicolchicine is a cyclobutane dimer of β-lumicolchicine (Figure 1).[28,29] This process highly depends on the solvent polarity and can be connected to the formation of a complex with a solvent in the ground state.[30,31]

Colchicine photoisomers differ from the parent compound in physical and biological properties. The rearrangement of methyl

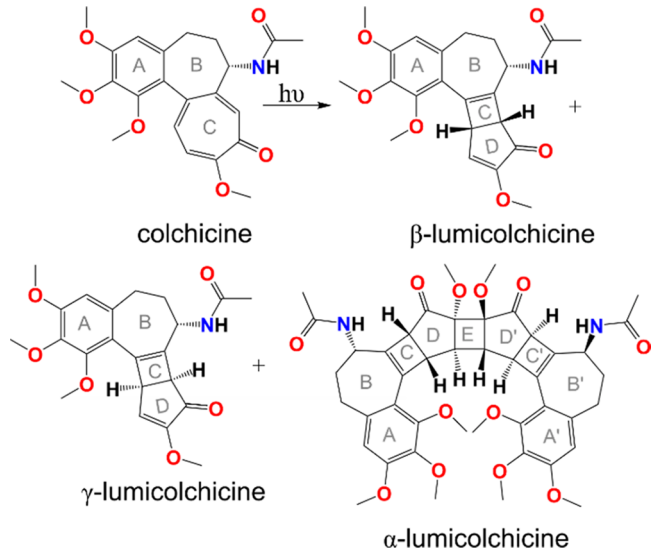

Figure 1. Structural formula of colchicine and its photoisomers: α-, β and γ-lumicolchicines.

Special Issue: Natural Products: An Era of Discovery in Organic Chemistry

Received: October 25, 2020
Published: December 22, 2020

https://dx.doi.org/10.1021/acs.joc.0c02507
J. Org. Chem. 2021, 86, 11029−11039

Scheme 1. Syntheses of Novel Colchicine Derivatives[a]

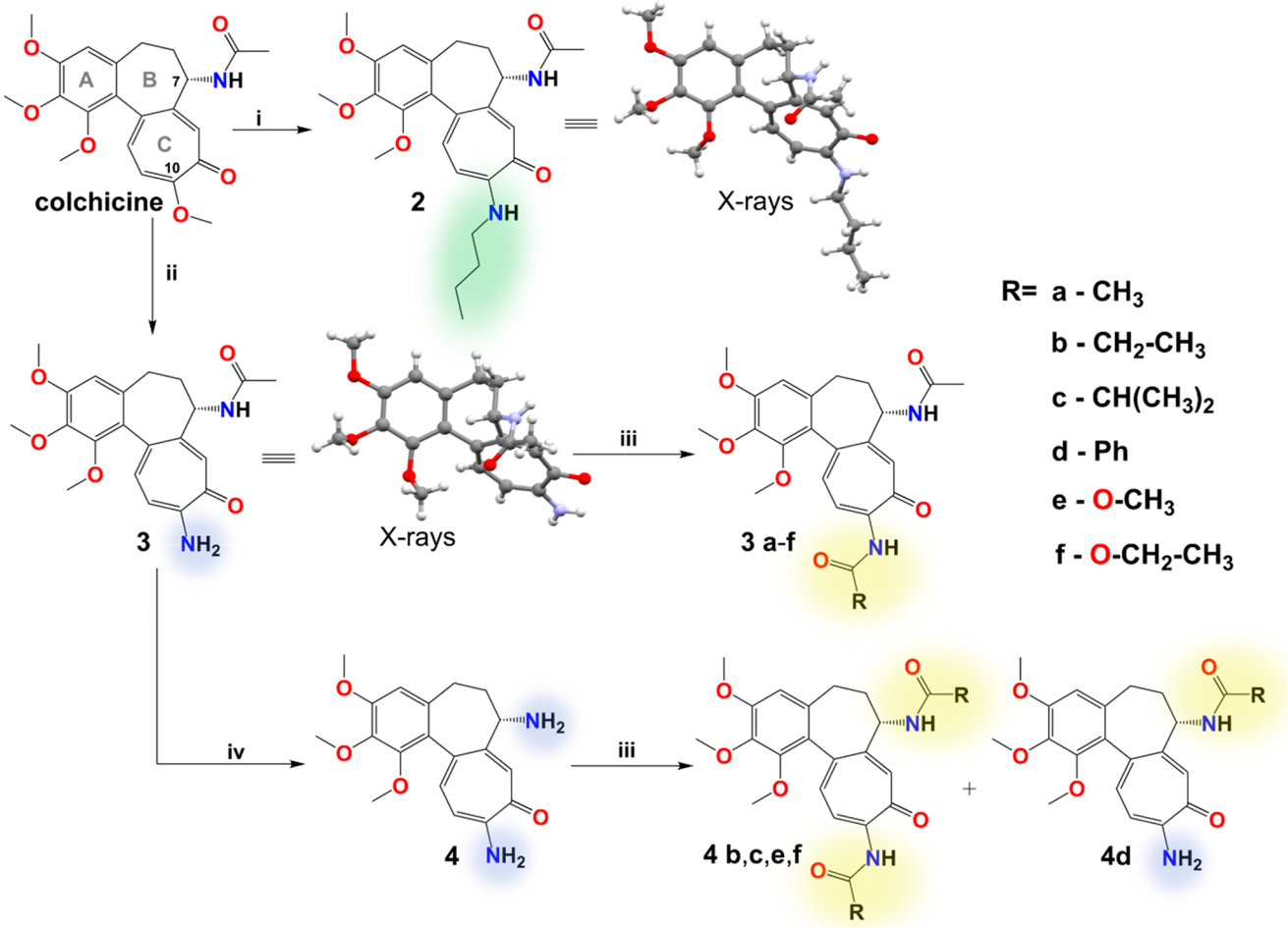

[a]Reagents and conditions: (i) *n*-butylamine, CH_3CN, reflux, 24 h; (ii) ammonia solution, CH_3CN, reflux, 24 h; (iii) DCM, Et_3N, respective acyl chloride/chloroformate, 0 °C → room temperature, 24 h; (iv) 4M HCl, MeOH, 90 °C, 72 h; the molecular structures of **2** and **3** are illustrated by their ball-and-stick models determined by X-ray diffraction, and denoted "X-rays".

tropolone ring C of colchicine to a conjugated 4- and 5-membered ring system prevents tubulin binding and mitosis arrest, which deactivates the therapeutic potency.[32,33] This is important from a clinical point of view, as considerable amounts of lumicolchicine were found in clear-glass ampules filled with colchicine for intravenous injections.[32] Studies on colchicine photoisomerization have been reported,[30,32−34] but the influence of different substituents on colchicine photosensitivity has not been investigated. It has been reported that the colchiceine (C10-demethylated colchicine analogue) undergoes photoisomerization similarly as colchicine, whereas thiocolchicine (C10-thiomethyl analogue) is resistant to UV irradiation. This information suggests that photostability of colchicine derivatives depends on the C-ring substituents.[29,34−36]

So far, the chemical modifications of colchicine have been mostly aimed at reducing its toxicity and increasing its bioavailability, while the improvement of its photostability has been neglected. Herein, we present the mechanism of the sun or/and UV irradiation induced rearrangement for a series of mono- and double-modified *N*-substituted colchicines at the C7 and C10 positions, as well as the analysis of biological activity of these new derivatives. Furthermore, we provide for the first time molecular structures of *β*-lumicolchicine and two *N*-substituted *β*-lumiderivatives, determined by single-crystal X-ray diffraction.

RESULTS AND DISCUSSION

The synthetic route for novel *N*-substituted colchicine derivatives is presented in Scheme 1. Compounds **2** and **3** were obtained quantitatively by refluxing colchicine with an excess of *n*-butylamine or aqueous ammonia solution (i, ii), respectively. The structures of these compounds were verified by the disappearance of the characteristic signal assigned to the C10 methoxy group at 56.5 ppm in the ^{13}C NMR spectrum of colchicine as well as by the X-ray analysis of the obtained single crystals from the solutions of **2** and **3** in chloroform/acetone 1:1 mixture (Scheme 1). The hydrolysis of **3** with 4 M HCl (iv) yielded compound **4** with two free amino groups at C7 and C10, traced by the disappearance of C7 acetyl group signals at 168.4 and 22.6 ppm present in the ^{13}C NMR spectra of colchicine. Single-modified derivatives **3a−f** and **4d**, as well as double-modified derivatives **4b,c,e,f**, were obtained by treating compounds **3** and **4** with appropriate acyl chlorides or chloroformates (iii). In the case of **4d**, the substituent was introduced only at the C7 position, while the amino group at the C10 remained free. The synthesized compounds were characterized by the ^{13}C NMR spectra, where one additional signal assigned to the carbonyl atom was observed for **3a−f** and **4d**, while two additional signals were noted for compounds **4b,c,e,f**.

https://dx.doi.org/10.1021/acs.joc.0c02507
J. Org. Chem. 2021, 86, 11029−11039

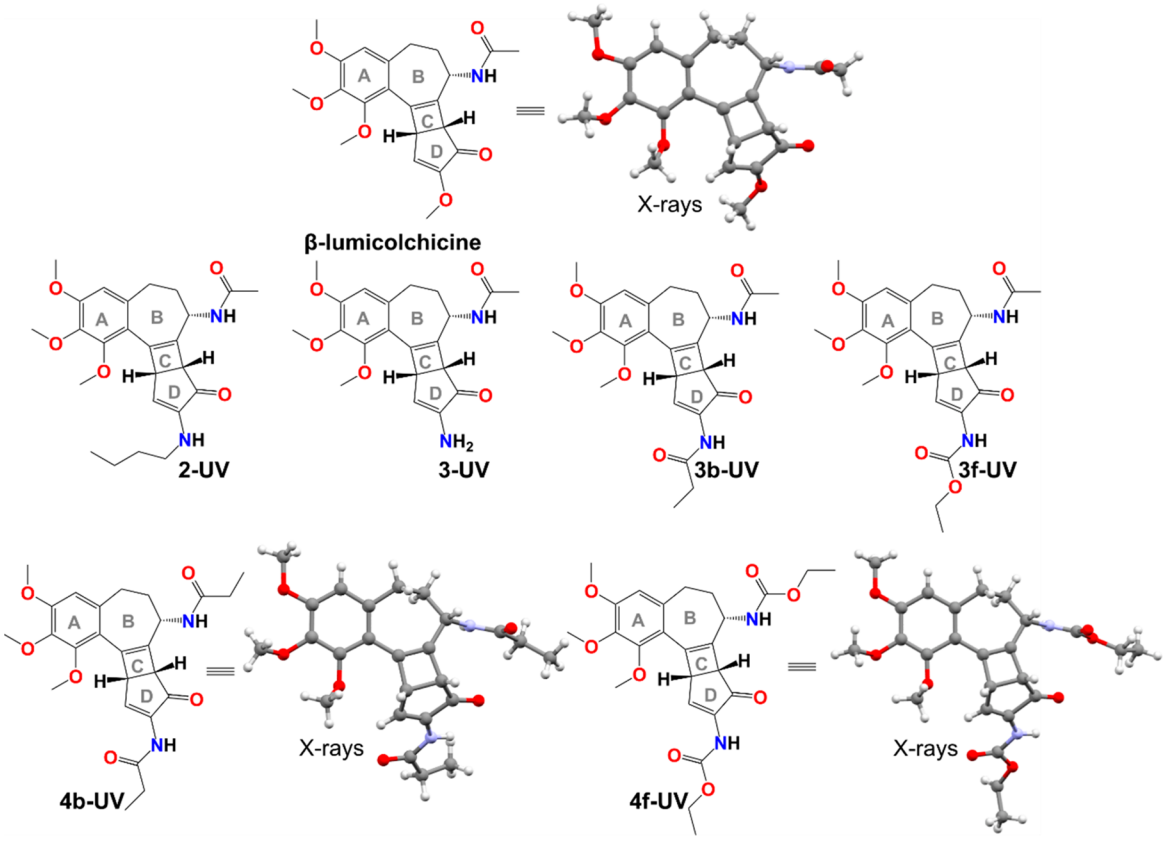

Figure 2. Structures of obtained β-lumicolchicine and its N-substituted derivatives (**2-UV**, **3-UV**, **3b-UV**, **3f-UV**, **4b-UV**, **4f-UV**); the molecular structures of β-lumicolchicine, **4b-UV**, and **4f-UV** are illustrated by their ball-and-stick models, determined by X-ray diffraction, and denoted "X-rays". The single crystals were obtained from the solutions of β-lumicolchicine, **4b-UV**, and **4f-UV** in chloroform/acetone 1:1 mixture.

Single crystals suitable for X-ray diffraction were obtained from the solutions of **4b** and **4f** in a chloroform/acetone 1:1 mixture. Surprisingly, the 5-day long crystallizations in transparent glass tubes led to photoproduct precipitation. The structures of the recovered crystals were no longer those of compounds **4b** and **4f**, but their photoisomers **4b-UV** and **4f-UV** (Figure 2). Remarkably, indirect sunlight was sufficient to induce migration of the C8−C14 and C12−C13 double bond and subsequent rearrangement of the tropolone ring C into 4- and 5-membered rings. Compounds **4b-UV** and **4f-UV** remain chiral and crystallize in acentrosymmetric space groups $P2_12_12_1$ and $P2_1$ respectively.

Photoinduced rearrangement of colchicine can lead to two possible stereochemical forms, β- and γ-lumicolchicine (Figure 1). Two stereoisomeric forms are possible, with the C7-substituent and the five-membered ring either in cis or trans configuration to each other, across the system of the four-membered ring nearly coplanar with rings A and B.[37] Only in the cis isomer of β-lumicolchicine, the intramolecular H-bond can link the carbonyl group of ring D with the amide or carbamate group of ring B in **4b-UV** or **4f-UV**.[37] In γ-lumicolchicine, this intramolecular H-bond is not possible. In the crystal structure of **4b-UV**, the H-bond between carbonyl O4 and amide N1 is 3.309 Å long; in **4f-UV** the H-bond of carbonyl O4 involves both N1 and O6 atoms from the carbamate substituent, and the O4···N1 and O4···O6 distances are 3.309 and 3.264 Å, respectively. As expected, the light-induced rearrangement retains the *S*-configuration at C7 but differentiates the photoproducts due to the bridging modes in tropolone ring C.

In order to obtain more quantitative description of photorearrangement of colchicine derivatives, we applied a high-pressure mercury lamp for illuminating the methanol solutions of compounds **4b** and **4f**. Reactions were carried out until the disappearance of the starting material (SM) on the TLC plate, followed by a change in the illuminated solution color from light-yellow to dark-brown or green. This method is convenient for measuring the time required for the full decay of the starting material. Hence, the exposure times in Table 1 correspond to the full conversions. The full conversion of **4b** into **4b-UV** was observed after 9 h, while the reaction from **4f** to **4f-UV** took only 4 h.

To confirm our observations, we decided to further illuminate the methanol solutions of derivatives **2**, **3**, **3b**, and **3f**. The illumination required for the photoisomerization of mono-modified **3b** and **3f**, bearing the same substituents at C10 as **4b** and **4f**, but with the acetamide group at C7, differed significantly.

Table 1. Illumination Times and Isolation Yields of Novel β-Lumiderivatives of Colchicine

starting material	exposure time (h)	isolation yield (%)
colchicine	4	44
2	6	37
3	6	61
3b	12	41
3f	4	52
4b	9	33
4f	4	31

https://dx.doi.org/10.1021/acs.joc.0c02507
J. Org. Chem. 2021, 86, 11029−11039

The conversion of **3b** to **3b-UV** required 12 h, while the reaction of **3f** to **3f-UV** took only 4 h, similarly as the **4f** → **4f-UV** reaction. The 3-times longer reaction time and longer irradiation for **3b** → **3b-UV**, compared to **3f** → **3f-UV**, is likely to be related to the effect of the amide group at C10 stabilizing the tropolone ring C. The irradiation of compounds **2** and **3**, with *n*-butylamine and free amine group at C10, respectively, took 6 h in both cases, in contrast to the required conversion time of 4 h for unmodified colchicine. The exposure times of starting materials and isolation yields for all the above-mentioned reactions are collected in Table 1.

To elucidate the mechanism of the rearrangement of *N*-substituted colchicine derivatives, we conducted additional time-resolved photochemical studies. The femtosecond flash-photolysis technique allowed observation of excited singlet-state transient absorption spectra ($S_1 \rightarrow S_n$, $S_2 \rightarrow S_n$) and excited-state dynamics ($S_1 \rightarrow S_0$) of colchicine derivatives in MeOH. The transient absorption spectra of MeOH solutions of **2** and **3** were recorded at room temperature, pumped at 330 nm, and probed by a delayed femtosecond pulsed light continuum (see Supporting Information for the experimental details). As can be seen in Figure 3, the spectra of compound **2** at different time delays were found to be a combination of ground-state bleaching, excited state $S_1 \rightarrow S_n$ and $S_2 \rightarrow S_n$ transient absorption, with some minor contribution of stimulated emission. The excited-state dynamics have been analyzed in different spectral regions as discussed in details below.

After a pulse excitation (330 nm, 80 fs) of MeOH solution of **2**, the broad absorption band at around 600 nm was observed. As can be seen in Figure 3, this initially formed absorption rapidly decays with a lifetime of $\tau_{1a} = 2.1 \pm 0.5$ ps, and a new, much stronger absorption band at 430 nm builds up with the same kinetics (growth fitting gives $\tau_1 = 1.9 \pm 0.6$ ps) followed by its decay with a lifetime of $\tau_2 = 29.1 \pm 2.0$ ps. The ground-state absorption bleach monitored at 356 nm was found to recover with exactly the same kinetics as visualized in Figure 3. After about 200 ps, the transient absorption signals decay to the initial signal level proving that no long-lived species (e.g., triplet excited state or free radicals) are generated and the ground state of **2** is completely recovered. The set of transient absorption spectra taken at different time delays (from subpicoseconds to 150 ps) is shown in Figure 3. The initial short-lived transient signal observed at around 600 nm can be assigned to the $S_2 \rightarrow S_n$ absorption of **2** quickly relaxing and populating a more stable S_1 state. Since in our experiment we used a relatively short excitation wavelength (330 nm), it is quite likely to excite directly to state S_2 or higher, any of which rapidly converts back to S_1.

The transient absorption spectra of compound **3** taken at different time delays following the 330 nm excitation pulse are shown in Figure 4. The most immediate broad absorption peaked around 530 nm decays with lifetime $\tau_1 = 1.7 \pm 0.5$ ps, and this feature can be assigned to the $S_2 \rightarrow S_n$ transient absorption. This ultrafast decay is followed by the growth of another absorption band ($\tau_{1a} = 1.6 \pm 0.7$ ps) peaking around 430 nm, subsequently decaying with lifetime $\tau_2 = 15.4 \pm 1.2$ ps, and this absorption can be assigned to $S_1 \rightarrow S_n$ absorption. The negative signal is attributed to the ground state bleach and, as can be seen in Figure 4, both the negative (ground state S_0 depletion) and positive (S_1 transient absorption) signals are fully recovered after ca. 100 ps and they both decay with the same kinetics. Moreover, there are no absorption signals for these decays, which would suggest a triplet formation.

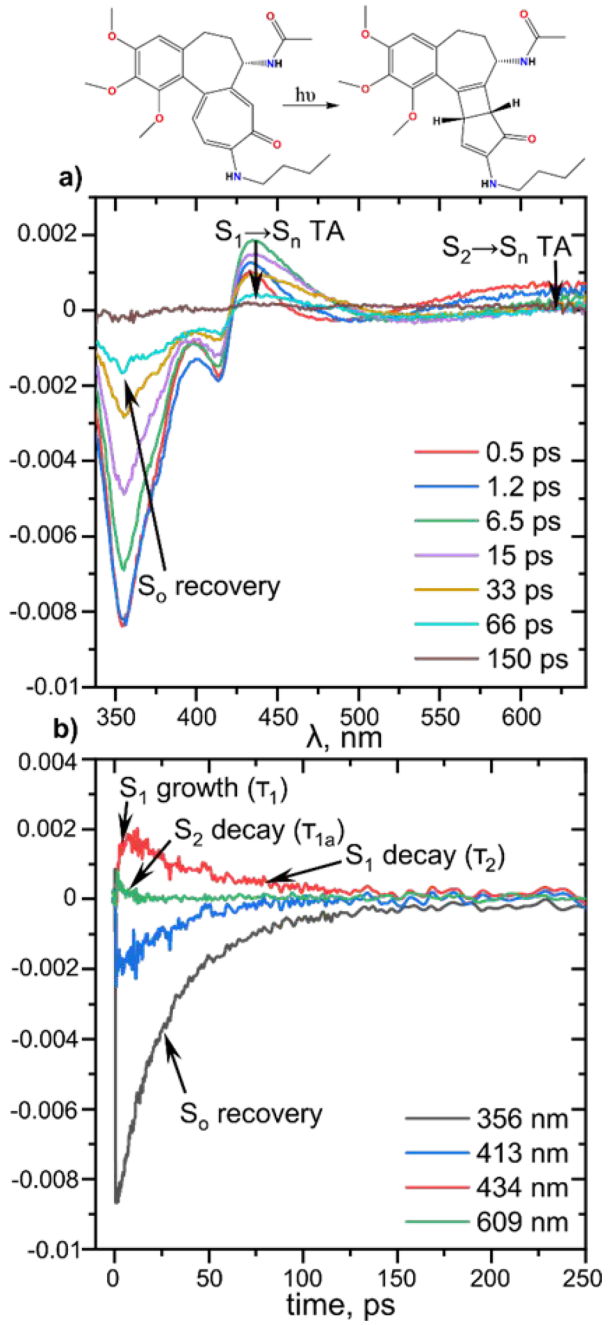

Figure 3. Absorption dynamics of **2** after 330 nm pulse laser excitation. Kinetic traces at selected wavelengths (b) and the set of transient absorption spectra (a) monitored at different time intervals after laser excitation of **2** in MeOH. $\tau_1 = 1.9 \pm 0.6$ ps (growth of S_1 TA); $\tau_{1a} = 2.1 \pm 0.6$ ps (decay of S_2 TA); $\tau_2 = 29.1 \pm 2.0$ ps.

The fast decay of the lowest excited singlet state S_1 (29 and 15 ps for **2** and **3**, respectively) can be attributed to the partly reversible excited-state intramolecular proton transfer (ESIPT) process occurring from the singlet excited state, followed by the photoisomerization of the compound. There was no indication of the triplet-state formation, as the ground-state absorption was recovered in less than 100 ps after the excitation pulse. In the ESIPT process, a proton is transferred from a donor to the proton acceptor and hydrogen-bonding interaction is the driving force for the reaction.[38−40] Thus, the H-bond strength plays a crucial role in the energetics and dynamics of the proton-transfer processes. In the investigated systems of *N*-substituted

https://dx.doi.org/10.1021/acs.joc.0c02507
J. Org. Chem. 2021, 86, 11029−11039

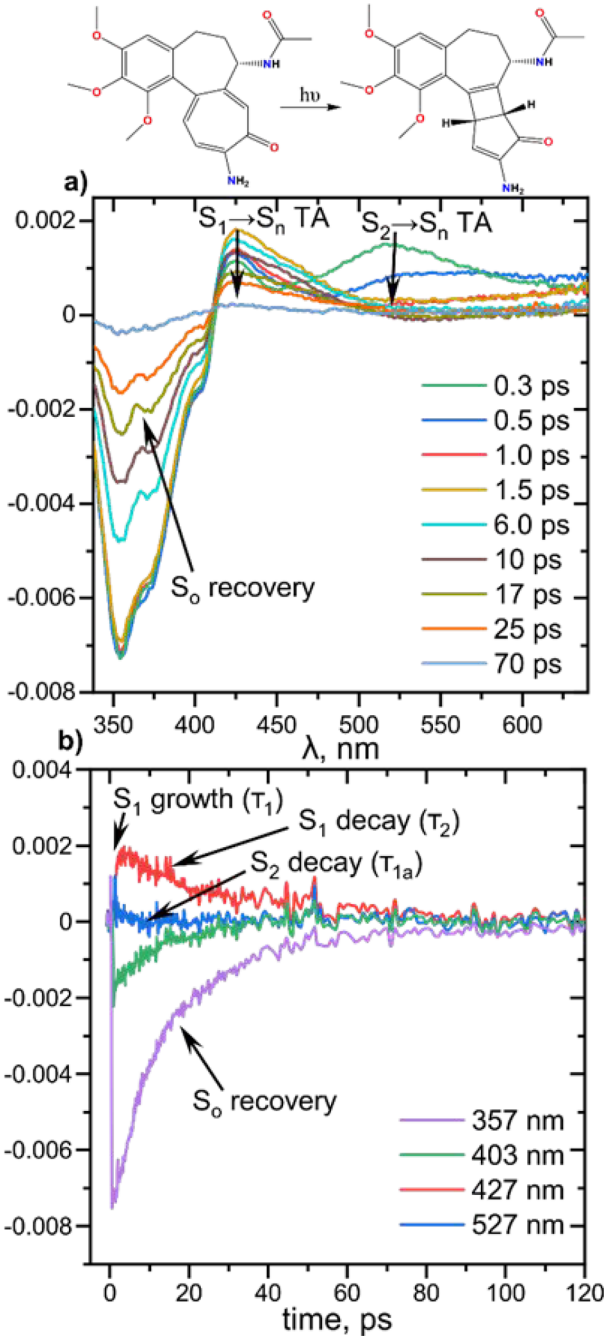

Figure 4. Absorption dynamics of **3** after 330 nm pulse laser excitation. Kinetic traces at selected wavelengths (b) and the set of transient absorption spectra (a) monitored at different time delays following 330 nm excitation of **3** in MeOH. Lifetmes $\tau_1 = 1.7 \pm 0.5$ ps; $\tau_{1a} = 1.6 \pm 0.7$ ps; $\tau_2 = 15.4 \pm 1.2$ ps.

colchicines, such intramolecular proton transfer in 5-membered-ring hydrogen-bonded system can be formed at C9 carbonyl atom, ultimately leading to photoisomerization (Figure 5).[40] This reasoning clearly explains the lack of photoreactivity of thiocolchicine, which forms weak or no hydrogen bonds.[29,34,36]

The novel β-lumiderivatives were fully characterized by spectrometric and spectroscopic methods. As expected, there were no differences in ESI-MS spectra, as the lumiderivatives have the same mass as the unrearranged derivatives. There are clear differences between lumiderivatives and unrearranged derivatives in the IR and UV−vis spectra. In the UV−vis spectra,

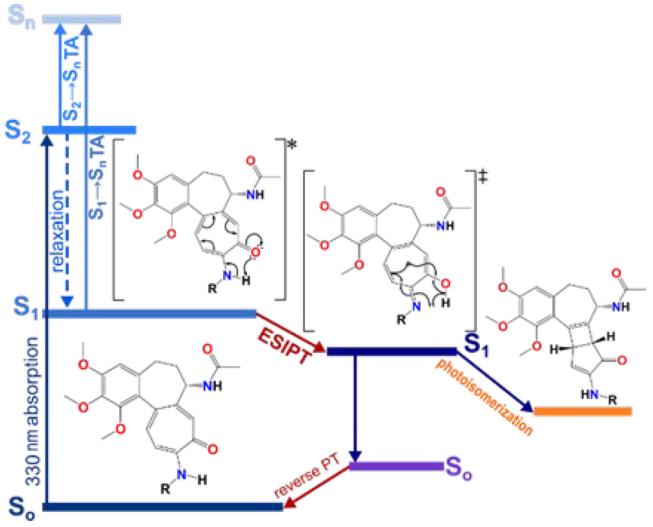

Figure 5. Photoisomerization mechanism scheme of N-substituted colchicines (TA, transient absorption; PT, proton transfer).

the disappearance of the tropolonic maximum absorption band around 350 nm was observed for all compounds and accompanied by the appearance of a new band around 280 nm, which confirmed the rearrangement of tropolone ring C.

Additionally, to observe how the UV−vis spectra evolve in time during irradiation, we exposed the methanol solution of **2** to UV radiation on an irradiation bench system (355 nm, CW laser, 20 mW). The absorption spectrum significantly changed after few minutes of exposure, suggesting a relatively fast photoismerization of the sample under UV light. As can be seen in Figure 6, at least three clearly defined isosbestic points are

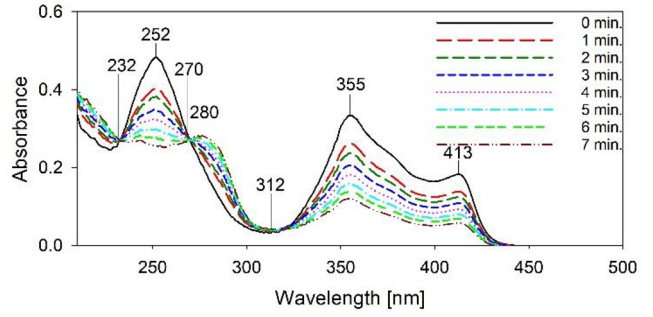

Figure 6. Cumulative effect of irradiation (355 nm) on absorption spectra of MeOH solution of **2** ($c = 2 \times 10^{-5}$ M). The quantum yield for photoisomerization of **2** is 0.004.

observed at 232, 270, and 312 nm, suggesting no secondary photochemical reactions (i.e., further photodegradation of the irradiation product). This is consistent with the proposed reaction scheme where no significant absorption at 355 nm is expected from the final isomeric photoproduct due to the lower number of aromatic π electrons in the conjugated system as compared to the starting reactant resulting in the blue-shift of the spectrum.

The most pronounced differences, which provided the clearest evidence for obtaining novel lumiderivatives (apart from the X-ray results), were observed in the NMR spectra. We used one- as well as two-dimensional NMR techniques (^{1}H−^{1}H COSY, ^{1}H−^{13}C HSQC, and ^{1}H−^{13}C HMBC) for assignment of signals of compounds **2** and **2-UV**. Almost all signals were

https://dx.doi.org/10.1021/acs.joc.0c02507
J. Org. Chem. 2021, 86, 11029−11039

shifted both in the ^{1}H and ^{13}C spectra when the rearrangement of ring C occurred. The most significant changes can be observed for the signal assigned to ring C, which shifted significantly due to the loss of aromaticity; e.g., the signal of C9 carbonyl atom shifted from 175.5 to 202.5 ppm. In Figure 7, we

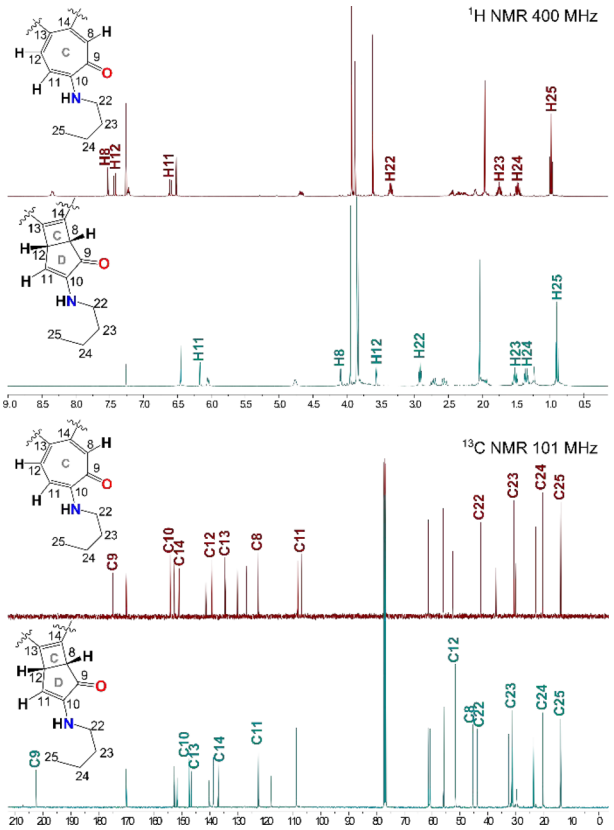

Figure 7. Stacked ^{1}H and ^{13}C NMR spectra of compounds **2** and **2-UV** in $CDCl_3$ with the signals assigned to rings C and D.

present the stacked spectra of compounds **2** and **2-UV** with the signals assigned to ring C. The copies of all spectra (^{1}H and ^{13}C NMR, IR, UV−vis) of all compounds studied are collected in the Supporting Information.

The biological activity of synthesized compounds was tested *in vitro* against three human cancer cell lines, human lung adenocarcinoma (A549), human breast adenocarcinoma (MCF-7), and human colon adenocarcinoma cell line (LoVo), as well as against normal murine embryonic fibroblast cell line (BALB/3T3) according to the previously published procedure.[41] The mean values of $IC_{50} \pm SD$ of the tested compounds are collected in Table 2. The structure−activity relationship of the synthesized series of mono- and double-modified colchicine derivatives at C7 and C10 position (Scheme 1) showed the strongest antiproliferative activity of compounds with small substituents at C10 position, e.g., **3**, **3a**, and **4d**. In the case of compounds **3**, **4**, and **4d**, which share a free amino group at the C10, their further modification and introduction of the diversified substituent at C7 influences their activity significantly. Compound **3** has an identical acetyl substituent at C7 as colchicine, and it exhibits comparable activity against all tested cell lines. Compound **4d**, with benzyl amide at C7, appears to be slightly less active than colchicine, which suggests that expanded substituent at C7 may affect interaction with the colchicine binding site (CBS) on the ß subunit of tubulin. Compound **4** with additional free amino group at the C7 is almost 100 times less active than **3**. In this case, high polarity of two free amine groups will improve water solubility but may hinder solubility in membranes and their penetration. This result is consistent with the previously reported derivatives deactylated at C7, which also exhibited low biological activity.[25,27] All *β*-lumiderivatives (*β*-lumicolchicine, **2-UV**, **3-UV**, **3b-UV**, **3f-UV**, **4b-UV**, **4f-UV**, Figure 2) are much less active than the regular derivatives. The activity of compound **3** and **3-UV** toward the A549 cell line deteriorated almost 10000 times, illustrating the unfavorable effects of light on the activity of colchicine derivatives. The rearrangement of ring C to conjugated 4- and 5-membered rings system in lumicolchicines most likely changes their position in colchicine binding site (CBS) and reduces their tubulin binding potency, which deactivates the biological activity of this class of colchicine derivatives.

CONCLUSIONS

We have developed an efficient method for the synthesis of mono- and double-modified *N*-substituted colchicine derivatives. Their recrystallization revealed the low stability of novel analogues **4b** and **4f** to sunlight, which prompted us to reproduce the photoeffects of sunlight on methanol solutions of **2**, **3**, **3b**, **3f**, **4b**, and **4f** using a high-pressure mercury lamp. The exposure time and irradiation doses varied depending on the character of the substituent at C7 and C10. Six novel *β*-lumiderivatives were obtained with isolation yields from 31 to 61% of compounds **4f-UV** and **3**, respectively. Detailed photochemical studies suggest that photoisomerization is associated with the partly reversible ESIPT process, during which intramolecular proton transfer in 5-membered-ring hydrogen-bonded system can occur at C9 carbonyl atom. The antiproliferative activity of the *β*-lumiderivatives decreased drastically when compared to those of the nonrearranged analogues, among which the most active derivatives were **3** and **4d**, with the free amino group at C10. These results indicate a new alley for controlling and improving the stability of colchicine APIs (active pharmaceutical ingredients) and in particular their resistance to the photoinduced conversions.

EXPERIMENTAL SECTION

General Methods. All precursors for the synthesis of colchicine derivatives and solvents were obtained from Merck or Fluka and were used as received without further purification. $CDCl_3$ and DMSO-d_6 spectral-grade solvents were stored over 3 Å molecular sieves for several days. All of the solvents used in flash chromatography were of HPLC grade (CHROMASOLV from Merck) and were used as received. Reaction mixtures were stirred using Teflon-coated magnetic stir bars. For reactions that require heating, a temperature-controlled heating block on a hot plate stirrer (Heidolph, MR-Hei Standard) was used. Reactions were monitored by thin-layer chromatography (TLC) using aluminum-backed plates (Merck 60 F254). TLC plates were visualized in UV light (254 nm). The ^{1}H, ^{13}C spectra were recorded on a Varian VNMR-S 400 MHz spectrometer using TMS as the internal standard in both cases. No window function or zero filling was used. ^{1}H NMR measurements of 1−14 (0.07 mol dm^{-3}) in $CDCl_3$ were carried out at an operating frequency of 402.64 MHz. The error of the chemical shift value was 0.01 ppm. The ^{13}C NMR spectra were recorded at an operating frequency 101.25 MHz. The error of chemical shift value was 0.1 ppm. All spectra were locked to a deuterium resonance of $CDCl_3$. The ESI (electrospray Ionization with the single quadrupole detection) mass spectra were recorded on a Waters/Micromass (Waters Corp., Manchester, UK) ZQ mass spectrometer equipped with a Harvard Apparatus syringe pump. The samples were prepared in dry acetonitrile (5×10^{-5} mol dm^{-3}). The sample was infused into the ESI source using

https://dx.doi.org/10.1021/acs.joc.0c02507
J. Org. Chem. 2021, 86, 11029−11039

Table 2. Antiproliferative Activity (IC_{50}) of Colchicine, Its Derivatives (2, 3, 3a−f, 4, and 4b−f) as Well as β-Lumiderivatives (β-Lumicolchicine, 2-UV, 3-UV, 3b-UV, 3f-UV, 4b-UV, and 4f-UV) Compared to the Antiproliferative Activity of Standard Anticancer Drugs Doxorubicin and Cisplatin and the Calculated Values of Selectivity Index (SI)[a]

	Compound	A549	SI	MCF-7	SI	LoVo	SI	BALB/3T3
		IC_{50} (μM)		IC_{50} (μM)		IC_{50} (μM)		IC_{50} (μM)
	2	0.85 ± 0.29	1.05	0.69 ± 0.30	1.29	0.63 ± 0.30	1.41	0.89 ± 0.35
	3	0.04 ± 0.03	0.73	0.01 ± 0.01	3.00	0.02 ± 0.01	1.50	0.03 ± 0.02
	3a	0.09 ± 0.01	0.78	0.09 ± 0.01	0.78	0.06 ± 0.01	1.17	0.07 ± 0.01
	3b	1.05 ± 0.22	1.09	0.93 ± 0.31	1.23	0.73 ± 0.35	1.57	1.14 ± 0.38
	3c	9.85 ± 0.55	0.67	6.96 ± 1.95	0.95	2.11± 1.12	3.14	6.62 ± 1.93
	3d	6.99 ± 1.20	0.30	5.99 ± 2.69	0.35	0.72 ± 0.19	2.91	2.10 ± 0.76
	3e	2.16 ± 0.94	0.60	1.12 ± 0.19	1.16	0.79 ± 0.08	1.64	1.30 ± 0.19
	3f	9.72 ± 0.22	0.83	6.06 ± 1.36	1.32	3.95 ± 0.81	2.03	8.03 ± 0.32
	4	1.68 ± 0.21	0.83	1.11 ± 0.17	1.26	0.99 ± 0.29	1.40	1.39 ± 0.49
	4b	5.69 ± 2.53	1.16	1.23 ± 0.60	5.35	1.56 ± 0.60	4.22	6.58 ± 1.53
	4c	12.64 ± 2.41	0.59	7.30 ± 1.53	1.03	6.36 ± 0.39	1.18	7.49 ± 2.80
	4d	0.15 ± 0.12	0.53	0.12 ± 0.08	0.67	0.08 ± 0.01	1.00	0.08 ± 0.01
	4e	6.91 ± 2.19	0.74	2.29 ± 1.00	2.23	0.92 ± 0.14	5.56	5.12 ± 0.98
	4f	9.50 ± 0.54	0.88	7.94 ± 2.23	1.05	5.01 ± 2.50	1.66	8.32 ± 4.08
β-lumiderivatives	2-UV	74.87 ± 3.58	1.53	73.00 ± 7.30	1.57	70.49 ± 7.64	1.62	114.41 ± 12.31
β-lumiderivatives	3-UV	99.60 ± 7.50	1.08	95.66 ± 7.86	1.13	82.44 ± 8.60	1.31	107.80 ± 2.32
β-lumiderivatives	3b-UV	107.37 ± 14.44	1.26	95.47 ± 7.67	1.41	85.17 ± 9.93	1.58	134.77 ± 20.06
β-lumiderivatives	3f-UV	83.82 ± 14.48	1.26	78.93 ± 9.56	1.34	94.63 ± 16.14	1.12	105.79 ± 11.59
β-lumiderivatives	4b-UV	85.71 ± 6.27	1.42	78.93 ± 0.75	1.54	76.01 ± 8.01	1.60	121.79 ± 20.71
β-lumiderivatives	4f-UV	15.71 ± 1.45	*	NA	*	15.86 ± 2.01	*	NA
β-lumiderivatives	β-lumicolch	61.10 ± 24.12	1.09	65.28 ± 18.06	1.02	20.65 ± 3.49	3.22	66.53 ± 34.55
	colchicine	0.07 ± 0.01	0.63	0.01 ± 0.01	4.30	0.01 ± 0.01	5.38	0.04 ± 0.01
	cisplatin	3.60 ± 0.25	0.81	3.05 ± 0.67	0.95	3.80 ± 0.28	0.77	2.91 ± 1.83
	doxorubicin	0.16 ± 0.03	0.25	0.15 ± 0.05	0.26	0.08 ± 0.03	0.49	0.04 ± 0.03

[a]The IC_{50} value is defined as the concentration of a compound at which 50% growth inhibition of cancer cells is observed. Human lung adenocarcinoma (A549), human breast adenocarcinoma (MCF-7), human colon adenocarcinoma cell line (LoVo), and normal murine embryonic fibroblast cell line (BALB/3T3). The SI (selectivity index) was calculated for each compound, using the formula SI = IC_{50} for normal cell line BALB/3T3/IC_{50} for the respective cancerous cell line. A beneficial SI > 1.0 indicates a drug with efficacy against tumor cells greater than the toxicity against normal cells. NA, compound inactive; at the highest concentration tested the inhibition of proliferation does not exceed 50%. *SI values were not calculated for inactive compounds.

a Harvard pump at a flow rate of 20 mL min^{-1}. The ESI source potentials were: capillary 3 kV, lens 0.5 kV, extractor 4 V. The standard ESI mass spectra were recorded at the cone voltages: 10 and 30 V. The source temperature was 120 °C and the desolvation temperature was 300 °C. Nitrogen was used as the nebulizing and desolvation gas at flow-rates of 100 dm^3/h. Mass spectra were acquired in the positive ion detection mode with unit mass resolution at a step of 1 m/z unit. The mass range for ESI experiments was from m/z = 100 to m/z = 1000, as well as from m/z = 200 to m/z = 1500. The elemental analysis of compounds was carried out on Vario ELIII (Elementar, Langenselbold, Germany).

Synthesis and Characterization of 2. To a solution of colchicine (400 mg; 1 mmol) in CH_3CN (10 mL) was added *n*-butylamine (0.5 mL, 5 mmol). The reaction mixture was stirred under reflux for 24 h (using a temperature controlled heating block on a hot plate-stirrer) while the reaction progress was determined by TLC. After that time, the solvent was evaporated under reduced pressure. The residue was purified by CombiFlash (0 → 10% methanol/EtOAc) to give **2**. Amorphous yellow solid, yield 94% (415 mg). ^{1}H NMR (400 MHz, $CDCl_3$): δ 8.35 (d, J = 6.9 Hz, 1H), 7.53 (s, 1H), 7.43 (d, J = 11.2 Hz, 1H), 7.23 (t, J = 5.7 Hz, 1H), 6.60 (d, J = 11.3 Hz, 1H), 6.52 (s, 1H), 4.74−4.65 (m, 1H), 3.93 (s, 3H), 3.89 (s, 3H), 3.62 (s, 3H), 3.35 (dd, J = 13.0, 7.0 Hz, 2H), 2.46 (dd, J = 12.4, 5.6 Hz, 1H), 2.41−2.32 (m, 1H), 2.32−2.21 (m, 1H), 2.18−2.07 (m, 1H), 1.98 (s, 3H), 1.81−1.70 (m, 2H), 1.54−1.43 (m, 2H), 0.98 (t, J = 7.3 Hz, 3H). ^{13}C{H} NMR (400 MHz, $CDCl_3$): δ 175.5, 169.9, 154.3, 152.8, 151.1, 151.0, 141.5, 139.4, 134.6, 130.3, 126.8, 122.6, 108.7, 107.1, 61.4, 61.3, 56.1, 52.6, 42.5, 37.2, 30.5, 30.0, 22.8, 20.3, 13.7. ESI-MS (m/z): $[M + H]^+$ 441, $[M + Na]^+$ 463, $[2M + Na]^+$ 903. Anal. Calcd for $C_{25}H_{32}N_2O_5$: C, 68.16; H, 7.32; N, 6.36. Found: C, 68.11; H 7.41; N, 6.29.

Synthesis and Characterization of 3. To a solution of **1** (400 mg; 1 mmol) in CH_3CN (10 mL) ammonia (25% aqueous solution, 0.5 mL, 7.35 mmol) was added. The reaction mixture was stirred under reflux for 24 h (using a temperature controlled heating block on a hot plate-stirrer), while the reaction progress was determined by TLC. After that time the solvent was evaporated under reduced pressure. The residue was purified by CombiFlash (0 → 50% acetone/chloroform) to give **3**. Amorphous yellow solid, yield 96% (370 mg). ^{1}H NMR (400 MHz, DMSO-d_6): δ 8.56 (d, J = 7.7 Hz, 1H), 7.13−7.06 (m, 2H), 6.89 (d, J = 11.1 Hz, 1H), 6.74 (s, 1H), 4.40−4.32 (m, 1H), 3.82 (s, 3H), 3.78 (s, 3H), 3.48 (s, 3H), 3.37 (s, 3H), 2.23−2.11 (m, 1H), 2.08−1.96 (m, 1H), 1.86 (s, 3H), 1.85−1.80 (m, 1H). ^{13}C{H} NMR (101 MHz,

https://dx.doi.org/10.1021/acs.joc.0c02507
J. Org. Chem. 2021, 86, 11029−11039

DMSO-d_6): δ 174.3, 168.4, 156.9, 152.3, 150.3, 149.4, 140.7, 138.0, 134.4, 128.8, 126.7, 123.6, 110.16, 107.5, 60.7, 60.5, 55.8, 51.4, 36.7, 29.4, 22.6. Anal. Calcd for $C_{21}H_{24}N_2O_5$: C, 65.61; H, 6.29; N, 7.29. Found: C, 65.57; H 6.37; N, 7.24.

General Route for Synthesis of Compounds 3a−f and 4b−f. To a solution of **3** or **4** (100 mg, 0.25 mmol) in dichloromethane (DCM, 10 mL) cooled to 0 °C, Et_3N (0.5 mL, 3.5 mmol) and respective acyl chloride or chloroformate were added (3.5 mmol). The mixture was first stirred at 0 °C for 30 min and then for the next 24 h at rt. Reaction progress was determined by TLC. Subsequently, the solvent was evaporated under reduced pressure and the residue was purified by CombiFlash (0 → 30% acetone/chloroform) to give respective compounds as amorphous yellow solids.

Characterization of 3a. The compound was prepared according to the general procedure, purified by CombiFlash (0 → 30% acetone/chloroform), to give **3a**. Amorphous yellow solid, yield 55% (61 mg). ^{1}H NMR (400 MHz, $CDCl_3$): δ 9.35 (s, 1H), 9.03 (d, J = 10.9 Hz, 1H), 7.60 (s, 1H), 7.46 (d, J = 10.9 Hz, 1H), 7.23 (d, J = 6.9 Hz, 1H), 6.52 (s, 1H), 4.71−4.56 (m, 1H), 3.92 (s, 3H), 3.89 (s, 3H), 3.62 (s, 3H), 2.52 (dd, J = 13.0, 6.1 Hz,1H), 2.31 (s, 3H), 2.30−2.20 (m, 1H), 1.98 (s, 3H), 1.90−1.79 (m, 1H). ^{13}C{H} NMR (101 MHz, $CDCl_3$): δ 177.7, 170.0, 169.7, 153.7, 152.8, 151.2, 145.4, 141.7, 139.6, 138.4, 133.9, 129.9, 125.6, 120.9, 107.2, 61.4, 61.3, 56.1, 52.5, 36.7, 29.8, 25.6, 22.8. ESI-MS (m/z): $[M + Na]^+$ 449, $[M + K]^+$ 465, $[2M + Na]^+$ 875, $[2M + K]^+$ 891. Anal. Calcd for $C_{23}H_{26}N_2O_6$: C, 64.78; H, 6.15; N, 6.57. Found: C, 64.81; H 6.10; N, 6.62.

Characterization of 3b. The compound was prepared according to the general procedure, purified by CombiFlash (0 → 30% acetone/chloroform), to give **3b**. Amorphous yellow solid, yield 58% (66 mg). ^{1}H NMR (400 MHz, $CDCl_3$): δ 9.38 (s, 1H), 9.05 (d, J = 10.9 Hz, 1H), 7.60 (s, 1H), 7.46 (d, J = 10.9 Hz, 1H), 6.52 (s, 1H), 4.69−4.62 (m, 1H), 3.92 (s, 3H), 3.88 (s, 3H), 3.62 (s, 3H), 2.55 (q, J = 7.5 Hz, 2H), 2.38−2.30 (m, 2H), 2.28−2.20 (m, 1H), 2.01−1.97 (m, 3H), 1.98 (s, 3H), 1.88−1.79 (m, 1H), 1.26 (t, 3H). ^{13}C{H} NMR (400 MHz, $CDCl_3$): δ 177.7, 173.7, 169.8, 153.6, 152.9, 151.2, 145.4, 141.6, 139.5, 138.5, 134.0, 129.8, 125.6, 120.9, 107.2, 61.4, 61.3, 56.1, 52.5, 36.6, 31.7, 29.7, 22.8, 9.3. ESI-MS (m/z): $[M + H]^+$ 441, $[M + Na]^+$ 463, $[M + K]^+$ 479, $[2M + Na]^+$ 903, $[2M + K]^+$ 919. Anal. Calcd $C_{24}H_{28}N_2O_6$ for C, 65.44; H, 6.41; N, 6.36. Found: C, 65.40; H 6.49; N, 6.31.

Characterization of 3c. The compound was prepared according to the general procedure, purified by CombiFlash (0 → 30% acetone/chloroform), to give **3c**. Amorphous yellow solid, yield 63% (74 mg). ^{1}H NMR (400 MHz, $CDCl_3$): δ 9.46 (s, 1H), 9.05 (d, J = 10.9 Hz, 1H), 7.59 (s, 1H), 7.46 (d, J = 10.9 Hz, 1H), 6.52 (s, 1H), 4.74−4.61 (m, 1H), 3.93 (s, 3H), 3.89 (s, 3H), 3.62 (s, 3H), 2.70 (dt, J = 13.8, 6.9 Hz, 1H), 2.51 (dd, J = 13.1, 5.9 Hz,1H), 2.40−2.31 (m, 1H), 2.29−2.20 (m, 1H), 1.99 (s, 3H), 1.88−1.79 (m, 2H), 1.28 (d, J = 6.9 Hz, 6H). ^{13}C{H} NMR (101 MHz, $CDCl_3$): δ 177.9, 177.0, 169.6, 153.6, 152.7, 151.2, 145.6, 141.6, 139.3, 138.4, 133.9, 129.7, 125.7, 120.8, 107.2, 61.4, 61.3, 56.1, 52.5, 37.5, 36.7, 29.7, 22.9, 19.5, 19.4. ESI-MS (m/z): $[M + H]^+$ 455, $[M + Na]^+$ 477, $[M + K]^+$ 493, $[2M + Na]^+$ 931, $[2M + K]^+$ 947. Anal. Calcd for $C_{25}H_{30}N_2O_6$: C, 66.06; H, 6.65; N, 6.16. Found: C, 66.16; H 6.71; N, 6.07.

Characterization of 3d. The compound was prepared according to the general procedure, purified by CombiFlash (0 → 30% acetone/chloroform), to give **3d**. Amorphous yellow solid, yield 35% (44 mg). ^{1}H NMR (400 MHz, $CDCl_3$): δ 10.33 (s, 1H), 9.23 (d, J = 10.9 Hz, 1H), 8.02−7.97 (m, 2H), 7.67 (s, 1H), 7.63−7.58 (m, 1H), 7.57−7.53 (m, 1H), 7.52 (d, J = 1.7 Hz, 2H), 6.54 (s, 1H), 4.74−4.67 (m, 1H), 3.95 (s, 3H), 3.90 (s, 3H), 3.66 (s, 3H), 2.54 (dd, J = 13.4, 6.0 Hz, 1H), 2.45−2.35 (m, 1H), 2.33−2.23 (m, 1H), 2.02 (s, 3H), 1.90−1.82 (m, 1H). ^{13}C{H} NMR (101 MHz, $CDCl_3$): δ 178.1, 169.6, 166.4, 153.7, 152.8, 151.3, 145.7, 141.8, 139.7, 138.4, 133.9, 132.5, 129.8, 128.9, 128.3, 127.5, 125.7, 121.0, 107.3, 61.5, 61.3, 56.1, 52.5, 36.9, 29.8, 23.0. ESI-MS (m/z): $[M + Na]^+$ 511. Anal. Calcd for $C_{28}H_{28}N_2O_6$: C, 68.84; H, 5.78; N, 5.73. Found: C, 68.75; H 5.80; N, 5.69.

Characterization of 3e. The compound was prepared according to the general procedure, purified by CombiFlash (0 → 30% acetone/chloroform), to give **3e**. Amorphous yellow solid, yield 49% (56 mg). ^{1}H NMR (400 MHz, $CDCl_3$): δ 8.93 (s, 1H), 8.67 (d, J = 10.9 Hz, 1H), 7.63 (d, J = 3.9 Hz, 1H), 7.48 (d, J = 11.0 Hz, 1H), 6.54 (s, 1H), 4.71−4.63(m,, 1H), 3.93 (s, 3H), 3.89 (s, 3H), 3.84 (s, 3H), 3.63 (s, 3H), 2.52(dd, J = 12.7, 5.5 Hz, 1H), 2.39−2.22 (m, 2H), 1.96 (s, 3H), 1.93−1.84 (m, 2H). ^{13}C{H} NMR (101 MHz, $CDCl_3$): δ 177.1, 169.8, 153.6, 153.1, 153.0, 151.2, 145.9, 141.6, 138.7, 138.2, 134.1, 129.2, 125.7, 119.2, 107.2, 61.5, 61.3, 56.1, 52.8, 52.6, 36.5, 29.8, 22.8.ESI-MS (m/z): $[M + H]^+$ 443, $[M + Na]^+$ 465, $[M + K]^+$ 481, $[2M + Na]^+$ 907, $[2M + K]^+$923. Anal. Calcd for $C_{23}H_{26}N_2O_7$: C, 62.43; H, 5.92; N, 6.33. Found: C, 62.36; H 5.98; N, 6.21.

Characterization of 3f. The compound was prepared according to the general procedure, purified by CombiFlash (0 → 30% acetone/chloroform), to give **3f**. Amorphous yellow solid, yield 61% (72 mg). ^{1}H NMR (400 MHz, $CDCl_3$): δ 8.89 (s, 1H), 8.68 (d, J = 10.9 Hz, 1H), 7.64−7.59 (m, 1H), 7.47 (d, J = 10.9 Hz, 1H), 6.52 (s, 1H), 4.67 (m, 1H), 4.28 (q, J = 7.1, 1.2 Hz, 2H), 3.93 (s, 3H), 3.89 (s, 3H), 3.63 (s, 3H), 2.52 (dd, J = 12.6, 5.4 Hz, 1H), 2.41−2.22 (m, 3H), 1.96 (s, 3H), 1.91−1.83 (m, 2H), 1.35 (t, J = 7.1 Hz, 3H). ^{13}C{H} NMR (101 MHz, $CDCl_3$): δ 177.2, 169.8, 153.6, 153.2, 152.9, 151.2, 146.1, 141.6, 138.5, 138.2, 134.1, 129.2, 125.7, 119.1, 107.2, 61.8, 61.5, 61.3, 56.1, 52.6, 36.6, 29.8, 22.8, 14.4. ESI-MS (m/z): $[M + H]^+$ 457, $[M + Na]^+$ 479, $[M + K]^+$ 495, $[2M + Na]^+$ 935, $[2M + K]^+$ 951. Anal. Calcd for $C_{24}H_{28}N_2O_7$: C, 63.15; H, 6.18; N, 6.14. Found: C, 63.07; H 6.22; N, 6.17.

Synthesis and Characterization of 4. To a solution of **3** (500 mg, 1.11 mmol) in MeOH (3 mL) was added 4 N HCl solution (5 mL). The mixture was stirred at 90 °C for 72 h. Reaction progress was determined by TLC. Subsequently the solvent was evaporated under reduced pressure. The residue was purified by CombiFlash (0 → 10% Methanol/EtOAc) to give **4** with yield 92%.[42] Amorphous yellow solid, yield 92% (410 mg). ^{1}H NMR (401 MHz, DMSO-d_6): δ 8.78 (s, 2H), 7.15 (d, J = 11.2 Hz, 1H), 7.05 (s, 1H), 6.98 (d, J = 11.2 Hz, 1H), 6.79 (s, 1H), 3.83 (s, 3H), 3.76 (s, 3H), 3.55 (s, 3H), 2.65−2.57 (m, 2H), 2.41−2.31 (m, 1H), 2.27−2.13 (m, 1H), 2.04−1.94 (m, 1H). ^{13}C{H} NMR (101 MHz, DMSO-d_6,): δ 173.9, 157.3, 152.7, 150.2, 143.0, 140.8, 138.9, 133.6, 127.8, 125.8, 123.0, 110.5, 107.6, 60.5, 55.9, 52.8, 35.7, 30.7, 28.8. ESI-MS (m/z): $[M + H]^+$ 343, $[M + Na]^+$ 356. Anal. Calcd for $C_{19}H_{22}N_2O_4$: C, 66.65; H, 6.48; N, 8.18. Found: C, 66.70; H 6.59; N, 8.15.

Characterization of 4b. The compound was prepared according to the general procedure, purified by CombiFlash (0 → 30% acetone/chloroform), to give **4b**. Amorphous yellow solid, yield 43% (57 mg). ^{1}H NMR (400 MHz, $CDCl_3$): δ 9.38 (s, 1H), 9.02 (d, J = 11.9, 1H), 7.51 (s, 1H), 7.44 (d, J = 11.9 Hz, 1H), 6.84−6.71 (m, 1H), 6.51 (s, 1H), 4.73−4.60 (m, 1H), 3.92 (s, 3H), 3.88 (s, 3H), 3.62 (s, 3H), 2.54 (q,J = 7.4, 2H), 2.40−2.30 (m, 1H), 2.25 (q, J = 7.6 Hz, 2H), 1.84−1.76 (m, 2H), 1.26 (t, J = 7.5 Hz,3H), 1.10 (t, J = 7.6 Hz, 3H). ^{13}C{H} NMR (101 MHz, $CDCl_3$): δ 177.8, 173.7, 173.2, 153.6, 152.5, 151.3, 145.4, 141.7, 139.2, 138.3, 133.9, 129.8, 125.7, 120.6, 107.2, 61.5, 61.3, 56.1, 52.2, 36.9, 31.7, 29.8, 29.3, 9.5, 9.3. ESI-MS (m/z): $[M + H]^+$ 455, $[M + Na]^+$ 477, $[M + K]^+$ 493. Anal. Calcd for $C_{25}H_{30}N_2O_6$: C, 66.06; H, 6.65; N, 6.16. Found: C, 66.01; H 6.61; N, 6.22.

Characterization of 4c. The compound was prepared according to the general procedure, purified by CombiFlash (0 → 30% acetone/chloroform), to give **4c**. Amorphous yellow solid, yield 57% (80 mg). ^{1}H NMR (400 MHz, $CDCl_3$): δ 9.47 (s, 1H), 9.03 (d, J = 10.9 Hz, 1H), 7.54 (d, J = 6.1 Hz, 1H), 7.45 (d, J = 10.9 Hz, 1H), 6.85−6.62 (m, 1H), 6.51 (s, 1H), 4.71−4.61 (m, 1H), 3.92 (s, 3H), 3.90 (s, 3H), 3.63 (s, 3H), 2.68 (hept, J = 6.9 Hz, 1H), 2.54−2.43 (m, 2H), 2.43−2.30 (m, 1H), 2.29−2.18 (m, 1H), 1.83−1.73 (m, 1H), 1.28 (d, J = 6.9 Hz,6H), 1.13 (d, J = 7.0 Hz,6H). ^{13}C{H} NMR (101 MHz, $CDCl_3$): δ 177.9, 176.9, 176.4, 153.6, 152.5, 151.3, 145.5, 141.7, 139.2, 138.3, 133.9, 129.8, 125.7, 120.6, 107.2, 61.5, 61.3, 56.1, 51.8, 37.5, 37.0, 35.3, 29.8, 19.49, 19.46, 19.44, 19.35. ESI-MS (m/z): $[M + Na]^+$ 505, $[M + K]^+$ 521, $[2M + Na]^+$987. Anal. Calcd for $C_{27}H_{34}N_2O_6$: C, 67.20; H, 7.10; N, 5.81; C, 67.29; H 7.07; N, 5.88.

Characterization of 4d. The compound was prepared according to the general procedure, purified by CombiFlash (0 → 30% acetone/chloroform), to give **4d**. Amorphous yellow solid, yield 33% (43 mg). ^{1}H NMR (400 MHz, $CDCl_3$): δ 8.28 (s, 1H), 7.81 (d, J = 7.6 Hz,2H),

https://dx.doi.org/10.1021/acs.joc.0c02507
J. Org. Chem. 2021, 86, 11029−11039

7.71 (s, 1H), 7.34 (d, J = 11.0 Hz, 1H), 7.22−7.15 (m, 2H), 6.88 (d, J = 11.0 Hz, 1H), 6.52 (s, 1H), 6.16 (s, 1H), 4.99−4.89 (m, 1H), 3.94 (s, 3H), 3.88 (s, 3H), 3.68 (s, 3H), 2.54−2.44 (m, 1H), 2.48 (dd, J = 12.9, 6.1 Hz,1H), 2.13−2.01 (m, 1H). ^{13}C{H} NMR (101 MHz, $CDCl_3$): δ 174.9, 167.1, 155.7, 153.0, 151.1, 150.8, 141.5, 138.9, 134.5, 133.7, 132.0, 131.3, 128.3, 127.1, 126.7, 125.4, 112.2, 107.3, 61.5, 61.4, 56.1, 52.8, 37.1, 30.1. ESI-MS (m/z): $[M + H]^+$ 447, $[M + Na]^+$ 469, $[M + K]^+$ 485, $[2M + Na]^+$ 915. Anal. Calcd for $C_{26}H_{26}N_2O_5$: C, 69.94; H, 5.87; N, 6.27. Found: C, 70.01; H 5.79; N, 6.35.

Characterization of 4e. The compound was prepared according to the general procedure, purified by CombiFlash (0 → 30% acetone/chloroform), to give **4e**. Amorphous yellow solid, yield 56% (75 mg). ^{1}H NMR (400 MHz, $CDCl_3$,): δ 8.95 (s, 1H), 8.62 (d, J = 10.9 Hz, 1H), 7.54 (s, 1H), 7.43 (d, J = 10.9 Hz, 1H), 6.53 (s, 1H), 5.26 (s, 1H), 4.52−4.40 (m, 1H), 3.94 (s, 3H), 3.90 (s, 3H), 3.83 (s, 3H), 3.61 (s, 3H), 3.60 (s, 3H), 2.52 (dd, J = 12.9, 5.8 Hz,1H), 2.44−2.22 (m, 3H), 1.80−1.69 (m, 1H). ^{13}C{H} NMR (101 MHz, $CDCl_3$): δ 177.4, 155.8, 153.8, 153.6, 151.7, 151.2, 146.0, 141.7, 137.8, 134.0, 129.7, 125.7, 118.6, 107.2, 61.4, 61.3, 56.1, 53.9, 52.7, 52.3, 37.4, 29.8, 29.7. ESI-MS (m/z): $[M + H]^+$ 459, $[M + Na]^+$ 481, $[M + K]^+$ 497. Anal. Calcd for $C_{23}H_{26}N_2O_8$: C, 60.26; H, 5.72; N, 6.11. Found: C, 60.20; H 5.64; N, 6.18.

Characterization of 4f. The compound was prepared according to the general procedure, purified by CombiFlash (0 → 30% acetone/chloroform), to give **4f**. Amorphous yellow solid, yield 62% (88 mg). ^{1}H NMR (400 MHz, $CDCl_3$): δ 8.91 (s, 1H), 8.61 (d, J = 10.9 Hz, 1H), 7.60 (s, 1H), 7.41 (d, J = 10.9 Hz, 1H), 6.52 (s, 1H), 5.64 (d, J = 7.1 Hz, 1H), 4.51−4.40 (m, 1H), 4.26 (q, J = 7.1 Hz, 2H), 3.96 (m, q, J = 6.9 Hz, 2H), 3.92 (s, 3H), 3.88 (s, 3H), 3.59 (s, 3H), 2.56 (dd, J = 12.6, 5.4 Hz,1H), 2.41−2.22 (m, 2H), 1.83−1.73 (m, 1H), 1.33 (t, J = 7.1 Hz, 3H), 1.12 (t, J = 7.1 Hz, 3H). ^{13}C{H} NMR (101 MHz, $CDCl_3$): δ 177.4, 155.4, 153.5, 153.3, 152.0, 151.2, 146.0, 141.6, 137.8, 134.1, 129.8, 125.7, 118.6, 107.2, 61.7, 61.3, 61.2, 61.0, 56.1, 53.7, 37.4, 29.8, 14.4, 14.3. ESI-MS (m/z): $[M + H]^+$ 487, $[M + Na]^+$ 509, $[M + K]^+$ 525, $[2M + Na]^+$ 995. Anal. Calcd for $C_{25}H_{30}N_2O_8$: C, 61.72; H, 6.22; N, 5.76. Found: C, 61.83; H 6.29; N, 5.72.

General Route for Photoisomers β-Lumicolchicine, 2-UV, 3-UV, 3b-UV, 3f-UV, 4b-UV, and 4f-UV. A solution of starting material (100 mg) in 5.5 mL of MeOH was irradiated in Pyrex glass tube, using a cylindrical photoreactor with an internal radiation source, equipped with a medium-pressure mercury lamp TQ 150W (Heraeus, Hanau, Germany), placed inside a cylindrical filter made of Pyrex glass with a wall thickness of 1.5 mm. The lamp with the filter was inside a quartz water jacket. The reaction was conducted until the disappearance of starting material on a TLC plate. After that the solvent was evaporated, and the crude product was purified by CombiFlash (0 → 30% acetone/chloroform) to give specifically β-isomers. The photograph of the photoreaction setup is shown in Figure S62.

Characterization of Photoisomer β-Lumicolchicine. The compound was prepared according to the general procedure, purified by CombiFlash (0 → 30% acetone/chloroform), to give β-lumicolchicine. Amorphous yellow solid, yield 44% (44 mg). ^{1}H NMR (400 MHz, $CDCl_3$): δ 6.65 (d, J = 3.2 Hz, 1H), 6.47 (s, 1H), 6.00 (d, J = 7.0 Hz, 1H), 4.84−4.76 (m, 1H), 4.10 (q, J = 2.9 Hz, 1H), 3.95 (s, 3H), 3.86 (s, 3H), 3.84 (s, 3H), 3.69 (s, 3H), 3.61 (dd, J = 2.6, 1.8 Hz, 1H), 2.75 (dd, J = 15.4, 9.1 Hz, 1H), 2.56 (dd, J = 15.4, 9.4 Hz, 1H), 2.05 (s, 3H), 2.03−1.96 (m, 1H), 1.96−1.88 (m, 1H). ^{13}C{H} NMR (101 MHz, $CDCl_3$): δ 200.9, 170.3, 157.7, 153.1, 151.7, 145.1, 140.2, 138.8, 137.2, 128.8, 117.6, 109.1, 61.4, 60.8, 56.8, 55.9, 51.42, 51.39, 43.2, 32.5, 31.3, 23.5. ESI-MS (m/z): $[M + Na]^+$ 422, $[2M + Na]^+$ 821. Anal. Calcd for $C_{22}H_{25}NO_6$: C, 66.15; H, 6.31; N, 3.51. Found: C, 66.03; H 6.45; N, 3.24.

Characterization of Photoisomer 2-UV. The compound was prepared according to the general procedure, purified by CombiFlash (0 → 30% acetone/chloroform), to give **2-UV**. Amorphous green solid, yield 37% (37 mg). ^{1}H NMR (400 MHz, $CDCl_3$): δ 6.45 (s, 1H), 6.17 (d, J = 3.3 Hz, 1H), 6.05 (d, J = 6.8 Hz, 1H), 4.78−4.73 (m, 1H), 4.09 (dd, J = 5.7, 2.9 Hz, 1H), 3.95 (s, 3H), 3.86 (s, 3H), 3.84 (s, 3H), 3.58−3.54 (m, 1H), 2.91 (t, J = 7.1 Hz, 2H), 2.72 (dd, J = 15.3, 8.8 Hz, 1H), 2.55 (dd, J = 15.3, 9.2 Hz, 1H), 2.04 (s, 3H), 2.01−1.86 (m, 2H), 1.56−1.47 (m, 2H), 1.41−1.29 (m, 2H), 0.89 (t, J = 7.3 Hz, 3H). ^{13}C{H} NMR (101 MHz, $CDCl_3$): δ 202.5, 170.1, 152.8, 151.7, 147.4, 146.7, 140.21, 138.7, 137.0, 122.5, 118.1, 108.9, 61.3, 60.7, 55.8, 51.6, 45.3, 43.8, 32.5, 31.3, 31.1, 23.5, 20.1, 13.9. ESI-MS (m/z): $[M + H]^+$ 441, $[M + Na]^+$ 463, $[2M + Na]^+$ 903. Anal. Calcd for $C_{25}H_{32}N_2O_5$: C, 68.16; H, 7.32; N, 6.36. Found: C, 68.08; H 7.45; N, 6.22.

Characterization of Photoisomer 3-UV. The compound was prepared according to the general procedure, purified by CombiFlash (0 → 30% acetone/chloroform), to give **3-UV**. Amorphous brown solid, yield 61% (61 mg). ^{1}H NMR (101 MHz, DMSO-d_6): δ 7.78 (d, J = 9.1 Hz, 1H), 6.68 (s, 1H), 6.24 (d, J = 3.2, 0.8 Hz, 1H), 4.72 (dd, J = 6.9, 1.8 Hz, 1H), 3.94 (dd, J = 5.5, 2.8 Hz 1H), 3.86 (s, 3H), 3.79 (s, 3H), 3.74 (s, 3H), 3.37 (s, 3H), 3.35 (dd, J = 2.8, 1.5 Hz, 1H), 2.69 (dd, J = 7.0, 3.6 Hz, 2H), 1.81 (s, 3H), 1.81−1.67 (m, 2H). ^{13}C{H} NMR (101 MHz, DMSO-d_6): δ 200.3, 168.3, 152.2, 151.3, 146.6, 144.6, 139.8, 139.6, 138.6, 123.7, 118.0, 109.3, 61.1, 60.3, 55.7, 50.8, 48.6, 44.2, 31.9, 31.6, 22.9 ppm. ESI-MS (m/z): $[M + Na]^+$ 407, $[2M + Na]^+$ 791. Anal. Calcd for $C_{21}H_{24}N_2O_5$: C, 65.61; H, 6.29; N, 7.29. Found: C, 65.68; H 6.24; N, 7.32.

Characterization of Photoisomer 3b-UV. The compound was prepared according to the general procedure, purified by CombiFlash (0 → 30% acetone/chloroform), to give **3b-UV**. Amorphous orange solid, yield 41% (41 mg). ^{1}H NMR (400 MHz, $CDCl_3$): δ 8.02 (d, J = 3.1 Hz, 1H), 7.7 (s, 1H), 6.38 (s, 1H), 5.82−5.76 (m, 1H), 4.81−4.74 (m, 1H), 4.21 (dd, J = 5.3, 2.7 Hz, 1H), 3.93 (s, 3H), 3.78 (s, 3H), 3.77 (s, 3H), 3.52 (dd, J = 2.6, 1.6 Hz, 1H), 2.69 (dd, J = 15.4, 9.2 Hz, 1H), 2.57−2.49 (m, 2H), 2.34−2.26 (m, 2H), 1.99 (s, 3H), 1.91−1.82 (m, 2H), 1.13 (t, J = 7.5, Hz, 3H). ^{13}C{H} NMR (101 MHz, $CDCl_3$): δ 201.2, 172.3, 169.9, 153.2, 152.0, 145.3, 141.5, 140.2, 138.5, 137.3, 136.7, 117.5, 108.8, 61.1, 60.7, 55.9, 51.2, 50.4, 46.8, 32.4, 31.3, 29.9, 29.6, 23.5, 9.2. ESI-MS (m/z): $[M + Na]^+$ 463, $[2M + Na]^+$ 903. Anal. Calcd for $C_{24}H_{28}N_2O_6$: C, 65.44; H, 6.41; N, 6.36. Found: C, 65.48; H 6.52; N, 6.27.

Characterization of Photoisomer 3f-UV. The compound was prepared according to the general procedure, purified by CombiFlash (0 → 30% acetone/chloroform), to give **3f-UV**. Amorphous beige solid, yield 52% (52%). ^{1}H NMR (400 MHz, $CDCl_3$): δ 7.71−7.60 (m, 1H), 6.75 (s, 1H), 6.38 (s, 1H), 5.82 (d, J = 7.2 Hz, 1H), 4.80−4.70 (m, 1H), 4.18 (dd, J = 5.5, 2.7 Hz, 1H), 4.11 (q, J = 7.1 Hz, 2H), 3.92 (s, 3H), 3.77 (s, 3H), 3.81 (s, 3H), 3.54−3.51 (m, 1H), 2.67 (dd, J = 15.4, 9.1 Hz, 1H), 2.50 (dd, J = 15.4, 9.5 Hz, 1H), 1.97 (s, 3H), 1.89−1.80 (m, 2H), 1.27−1.21 (m, 3H). ^{13}C{H} NMR (101 MHz, $CDCl_3$): δ 200.4, 169.9, 153.3, 153.1, 151.9, 145.3, 140.1, 138.6, 138.5, 137.7, 136.8, 117.5, 108.8, 61.6, 61.1, 60.7, 55.8, 51.1, 50.6, 46.3, 32.4, 31.3, 23.4, 14.3. ESI-MS (m/z): $[M + Na]^+$ 479, $[2M + Na]^+$ 935. Anal. Calcd for $C_{24}H_{28}N_2O_7$: C, 63.15; H, 6.18; N, 6.14. Found: C, 63.11; H, 6.27; N, 6.10.

Characterization of Photoisomer 4b-UV. The compound was prepared according to the general procedure, purified by CombiFlash (0 → 30% acetone/chloroform), to give **4b-UV**. Amorphous yellow solid, yield 33% (33 mg). ^{1}H NMR (400 MHz, $CDCl_3$): δ 8.07 (d, J = 3.1 Hz, 1H), 7.40 (s, 1H), 6.43 (s, 1H), 5.74 (d, J = 7.3 Hz, 1H), 4.88−4.80 (m, 1H), 4.27 (dd, J = 5.5, 2.8 Hz,1H), 3.98 (s, 3H), 3.83 (s, 3H), 3.82 (s, 3H), 3.57 (dd, J = 2.7, 1.7 Hz, 1H), 2.74 (dd, J = 15.3, 9.2 Hz, 1H), 2.59−2.50 (m, 1H), 2.35 (q, J = 7.5 Hz, 2H), 2.30−2.21 (m, 2H), 2.07−2.00 (m, 1H), 1.94−1.85 (m, 1H), 1.19 (m, 6H). ^{13}C{H} NMR (101 MHz, $CDCl_3$): δ 201.1, 173.5, 172.3, 153.2, 152.0, 145.3, 141.5, 140.2, 138.6, 137.3, 136.8, 117.5, 108.7, 61.1, 60.7, 55.9, 51.1, 50.4, 46.8, 32.4, 31.4, 29.9, 29.8, 9.5, 9.2. ESI-MS (m/z): $[M + Na]^+$ 477, $[2M + Na]^+$ 931. Anal. Calcd for $C_{25}H_{30}N_2O_6$: C, 66.06; H, 6.65; N, 6.16. Found: C, 65.98; H 6.72; N, 6.20.

Characterization of Photoisomer 4f-UV. The compound was prepared according to the general procedure, purified by CombiFlash (0 → 30% Acetone/Chloroform), to give **4f-UV**. Amorphous beige solid, yield 31% (31 mg). ^{1}H NMR (400 MHz, $CDCl_3$): δ 7.74−7.64 (m, 1H), 6.83 (s, 1H), 6.44 (s, 1H), 4.95 (d, J = 5.6 Hz, 1H), 4.58−4.52 (m, 1H), 4.25 (dd, J = 5.5, 2.7 Hz, 1H), 3.97 (s, 3H), 3.83 (s, 3H), 3.82 (s, 3H), 3.63−3.57 (m, 1H), 2.71 (dd, J = 15.3, 8.4 Hz, 1H), 2.52 (dd, J = 15.3, 9.3 Hz, 1H), 2.06−1.90 (m, 2H), 1.33−1.22 (m, 6H). ^{13}C{H} NMR (101 MHz, $CDCl_3$): δ 200.1, 155.9, 153.4, 153.1, 152.0, 145.5,

https://dx.doi.org/10.1021/acs.joc.0c02507
J. Org. Chem. 2021, 86, 11029−11039

140.2, 138.9, 137.8, 137.7, 137.0, 117.6, 108.7, 61.5, 61.1, 61.0, 60.7, 55.9, 52.3, 50.7, 46.3, 32.0, 31.8, 14.6, 14.4. ESI-MS (m/z): $[M + Na]^+$ 509, $[2M + Na]^+$ 995. Anal. Calcd for $C_{25}H_{30}N_2O_8$: C, 61.72; H, 6.22; N, 5.76. Found: C, 61.66; H 6.18; N, 5.83.

■ ASSOCIATED CONTENT

Supporting Information

The Supporting Information is available free of charge at https://pubs.acs.org/doi/10.1021/acs.joc.0c02507.

Detailed description of conducted antiproliferative assay, X-ray measurements with thermal ellipsoid plot for each crystal structure and crystallographic data, photochemical measurements, a photograph of the photoreaction setup, copies of ^1H and ^{13}C NMR, IR, and UV−vis spectra, a photograph of the reaction setup (PDF)

Accession Codes

CCDC 2033154−2033158 contain the supplementary crystallographic data for this paper. These data can be obtained free of charge via www.ccdc.cam.ac.uk/data_request/cif, or by emailing data_request@ccdc.cam.ac.uk, or by contacting The Cambridge Crystallographic Data Centre, 12 Union Road, Cambridge CB2 1EZ, UK; fax: +44 1223 336033.

■ AUTHOR INFORMATION

Corresponding Author

Adam Huczyński − *Faculty of Chemistry, Adam Mickiewicz University, 61-614 Poznań, Poland;* orcid.org/0000-0003-4770-215X; Phone: +48618291673; Email: adhucz@amu.edu.pl

Authors

Dominika Czerwonka − *Faculty of Chemistry, Adam Mickiewicz University, 61-614 Poznań, Poland;* orcid.org/0000-0002-8098-5975

Szymon Sobczak − *Faculty of Chemistry, Adam Mickiewicz University, 61-614 Poznań, Poland;* orcid.org/0000-0001-8234-2503

Tomasz Pędziński − *Faculty of Chemistry and Center for Advanced Technology, Adam Mickiewicz University, 61-614 Poznań, Poland;* orcid.org/0000-0002-4765-6264

Ewa Maj − *Hirszfeld Institute of Immunology and Experimental Therapy, Polish Academy of Sciences, 53-114 Wrocław, Poland;* orcid.org/0000-0001-5205-8712

Joanna Wietrzyk − *Hirszfeld Institute of Immunology and Experimental Therapy, Polish Academy of Sciences, 53-114 Wrocław, Poland;* orcid.org/0000-0003-4980-6606

Lech Celewicz − *Faculty of Chemistry, Adam Mickiewicz University, 61-614 Poznań, Poland;* orcid.org/0000-0001-6156-2523

Andrzej Katrusiak − *Faculty of Chemistry, Adam Mickiewicz University, 61-614 Poznań, Poland;* orcid.org/0000-0002-1439-7278

Complete contact information is available at: https://pubs.acs.org/10.1021/acs.joc.0c02507

Author Contributions

Conceptualization: D.C. and A.H.. Methodology: D.C., A.H., T.P, S.S., and E.M.. Validation: A.H., A.K., and J.W.. Investigation: D.C, T.P., S.S., and E.M. Resources: L.C., T.P., A.H., A.K., and J.W.. Data curation: D.C., S.S., and E.M. Writing—original draft preparation as well as TOC design: D.C. and S.S.. Writing—review and editing: D.C., A.H., A.K., and J.W. Visualization: D.C. Supervision: A.H.. Project administration: A.H.. Funding acquisition: A.H. All authors have read and agreed to the published version of the manuscript.

Funding

Financial support from grant of the Polish National Science Centre (NCN) (No. 2016/21/B/ST5/00111) is gratefully acknowledged. D.C. and S.S. acknowledge a scholarship (No. POWR. 03.02.00-00-I026/16 and POWR. 03.02.00-00-I023/17, respectively) cofinanced by the European Union through the European Social Fund under the Operational Program Knowledge Education Development. D.C. acknowledges the NCN for a doctoral scholarship ETIUDA (2020/36/T/ST4/00041).

Notes

The authors declare no competing financial interest.

■ ACKNOWLEDGMENTS

We are grateful to Greta Klejborowska for valuable suggestions.

■ REFERENCES

(1) Ahmad, I.; Ahmed, S.; Anwar, Z.; Sheraz, M. A.; Sikorski, M. Photostability and Photostabilization of Drugs and Drug Products. *International Journal of Photoenergy*; Hindawi Publishing Corp., 2016. DOI: 10.1155/2016/8135608.

(2) *Photostability of Drugs and Drug Formulations*, 2nd ed.; Hanne, Hj, Ed.https://www.routledge.com/Photostability-of-Drugs-and-Drug-Formulations/Tonnesen/p/book/9780367394103 (accessed 2020-09-21).

(3) Tønnesen, H. H. Formulation and Stability Testing of Photolabile Drugs. *Int. J. Pharm.* **2001**, *225* (1−2), 1−14.

(4) Slobodnick, A.; Shah, B.; Pillinger, M. H.; Krasnokutsky, S. Colchicine: Old and New. *Am. J. Med.* **2015**, *128*, 461−470.

(5) Khanna, D.; Fitzgerald, J. D.; Khanna, P. P.; Bae, S.; Singh, M. K.; Neogi, T.; Pillinger, M. H.; Merill, J.; Lee, S.; Prakash, S.; Kaldas, M.; Gogia, M.; Perez-Ruiz, F.; Taylor, W.; Lioté, F.; Choi, H.; Singh, J. A.; Dalbeth, N.; Kaplan, S.; Niyyar, V.; Jones, D.; Yarows, S. A.; Roessler, B.; Kerr, G.; King, C.; Levy, G.; Furst, D. E.; Edwards, N. L.; Mandell, B.; Schumacher, H. R.; Robbins, M.; Wenger, N.; Terkeltaub, R. 2012 American College of Rheumatology Guidelines for Management of Gout. Part 1: Systematic Nonpharmacologic and Pharmacologic Therapeutic Approaches to Hyperuricemia. *Arthritis Care Res.* **2012**, *64* (10), 1431−1446.

(6) Grattagliano, I.; Bonfrate, L.; Ruggiero, V.; Scaccianoce, G.; Palasciano, G.; Portincasa, P. Novel Therapeutics for the Treatment of Familial Mediterranean Fever: From Colchicine to Biologics. *Clin. Pharmacol. Ther.* **2013**, *95* (1), 89−97.

(7) Imazio, M.; Gaita, F.; Le Winter, M. Evaluation and Treatment of Pericarditis: A Systematic Review. *JAMA - Journal of the American Medical Association.* **2015**, *314*, 1498−1506.

(8) Vindya, N. G.; Sharma, N.; Yadav, M.; Ethiraj, K. R. Tubulins - The Target for Anticancer Therapy. *Curr. Top. Med. Chem.* **2015**, *15* (1), 73−82.

(9) Seligmann, J.; Twelves, C. Tubulin: An Example of Targeted Chemotherapy. *Future Med. Chem.* **2013**, *5*, 339−352.

(10) Katsetos, C. D.; Draber, P. Tubulins as Therapeutic Targets in Cancer: From Bench to Bedside. *Curr. Pharm. Des.* **2012**, *18* (19), 2778−2792.

(11) Cocco, G.; Chu, D. C. C.; Pandolfi, S. Colchicine in Clinical Medicine. A Guide for Internists. *Eur. J. Intern. Med.* **2010**, *21*, 503−508.

(12) Yang, L. P. H. Oral Colchicine (Colcrys®: In the Treatment and Prophylaxis of Gout. *Drugs* **2010**, *70*, 1603−1613.

(13) Avendaño, C.; Menéndez, J. C. *Medicinal Chemistry of Anticancer Drugs*; Elsevier, 2008. DOI: 10.1016/B978-0-444-52824-7.X0001-7.

(14) Kozaka, T.; Nakagawa-Goto, K.; Shi, Q.; Lai, C. Y.; Hamel, E.; Bastow, K. F.; Brossi, A.; Lee, K. H. Antitumor Agents 273. Design and

Synthesis of N-Alkyl-Thiocolchicinoids as Potential Antitumor Agents. *Bioorg. Med. Chem. Lett.* **2010**, *20* (14), 4091−4094.
(15) Kumar, A.; Sharma, P. R.; Mondhe, D. M. Potential Anticancer Role of Colchicine-Based Derivatives: An Overview. *Anti-Cancer Drugs* **2017**, *28*, 250−262.
(16) Johnson, L.; Goping, I. S.; Rieger, A.; Mane, J. Y.; Huzil, T.; Banerjee, A.; Luduena, R.; Hassani, B.; Winter, P.; Tuszynski, J. A. Novel Colchicine Derivatives and Their Anti-Cancer Activity. *Curr. Top. Med. Chem.* **2017**, DOI: 10.2174/1568026617666170104143618.
(17) Marzo-Mas, A.; Barbier, P.; Breuzard, G.; Allegro, D.; Falomir, E.; Murga, J.; Carda, M.; Peyrot, V.; Marco, J. A. Interactions of Long-Chain Homologues of Colchicine with Tubulin. *Eur. J. Med. Chem.* **2017**, *126*, 526−535.
(18) Chang, D. J.; Yoon, E. Y.; Lee, G. B.; Kim, S. O.; Kim, W. J.; Kim, Y. M.; Jung, J. W.; An, H.; Suh, Y. G. Design, Synthesis and Identification of Novel Colchicine-Derived Immunosuppressant. *Bioorg. Med. Chem. Lett.* **2009**, *19* (15), 4416−4420.
(19) Nicolaou, K. C.; Valiulin, R. A.; Pokorski, J. K.; Chang, V.; Chen, J. S. Bio-Inspired Synthesis and Biological Evaluation of a Colchicine-Related Compound Library. *Bioorg. Med. Chem. Lett.* **2012**, *22* (11), 3776−3780.
(20) Zhang, X.; Kong, Y.; Zhang, J.; Su, M.; Zhou, Y.; Zang, Y.; Li, J.; Chen, Y.; Fang, Y.; Zhang, X.; Lu, W. Design, Synthesis and Biological Evaluation of Colchicine Derivatives as Novel Tubulin and Histone Deacetylase Dual Inhibitors. *Eur. J. Med. Chem.* **2015**, *95*, 127−135.
(21) Yasobu, N.; Kitajima, M.; Kogure, N.; Shishido, Y.; Matsuzaki, T.; Nagaoka, M.; Takayama, H. Design, Synthesis, and Antitumor Activity of 4-Halocolchicines and Their pro-Drugs Activated by Cathepsin B. *ACS Med. Chem. Lett.* **2011**, *2* (5), 348−352.
(22) Shchegravina, E. S.; Maleev, A. A.; Ignatov, S. K.; Gracheva, I. A.; Stein, A.; Schmalz, H. G.; Gavryushin, A. E.; Zubareva, A. A.; Svirshchevskaya, E. V.; Fedorov, A. Y. Synthesis and Biological Evaluation of Novel Non-Racemic Indole-Containing Allocolchicinoids. *Eur. J. Med. Chem.* **2017**, *141*, 51−60.
(23) Nakagawa-Goto, K.; Chen, C. X.; Hamel, E.; Wu, C. C.; Bastow, K. F.; Brossi, A.; Lee, K. H. Antitumor Agents. Part 236: Synthesis of Water-Soluble Colchicine Derivatives. *Bioorg. Med. Chem. Lett.* **2005**, *15* (1), 235−238.
(24) Czerwonka, D.; Sobczak, S.; Maj, E.; Wietrzyk, J.; Katrusiak, A.; Huczyński, A. Synthesis and Antiproliferative Screening Of Novel Analogs of Regioselectively Demethylated Colchicine and Thiocolchicine. *Molecules* **2020**, *25* (5), 1180.
(25) Majcher, U.; Urbaniak, A.; Maj, E.; Moshari, M.; Delgado, M.; Wietrzyk, J.; Bartl, F.; Chambers, T. C.; Tuszynski, J. A.; Huczyński, A. Synthesis, Antiproliferative Activity and Molecular Docking of Thiocolchicine Urethanes. *Bioorg. Chem.* **2018**, *81*, 553−566.
(26) Huczyński, A.; Majcher, U.; Maj, E.; Wietrzyk, J.; Janczak, J.; Moshari, M.; Tuszynski, J. A.; Bartl, F. Synthesis, Antiproliferative Activity and Molecular Docking of Colchicine Derivatives. *Bioorg. Chem.* **2016**, *64*, 103−112.
(27) Klejborowska, G.; Urbaniak, A.; Preto, J.; Maj, E.; Moshari, M.; Wietrzyk, J.; Tuszynski, J. A.; Chambers, T. C.; Huczyński, A. Synthesis, Biological Evaluation and Molecular Docking Studies of New Amides of 4-Bromothiocolchicine as Anticancer Agents. *Bioorg. Med. Chem.* **2019**, *27*, 115144.
(28) Sabnis, D. D. Lumicolchicine as a Tool in the Study of Plant Microtubules: Some Biological Effects of Sequential Products Formed during Phototransformations of Colchicine. *J. Exp. Bot.* **1981**, *32* (1), 271−278.
(29) Bussotti, L.; Cacelli, I.; D'Auria, M.; Foggi, P.; Lesma, G.; Silvani, A.; Villani, V. Photochemical Isomerization of Colchicine and Thiocolchicine. *J. Phys. Chem. A* **2003**, *107* (43), 9079−9085.
(30) Roigt, H.; Leblanc, R. M. Processus Photophysiques Dans La Molécule de Colchicine. *Can. J. Chem.* **1973**, *51* (17), 2821−2827.
(31) Ghanem, R.; Baker, H.; Seif, M. A.; Al-Qawasmeh, R. A.; Mataneh, A. A.; Al-Gharabli, S. I. Photochemical Transformation of Colchicine: A Kinetic Study. *J. Solution Chem.* **2010**, *39* (4), 441−456.
(32) Sagorin, C.; Ertel, N. H.; Wallace, S. L. Photoisomerization of Colchicine. Loss of Significant Antimitotic Activity in Human Lymphocytes. *Arthritis Rheum.* **1972**, *15* (2), 213−217.
(33) Malawista, S. E.; Chang, Y. -H; Wilson, L. Lumicolchicine: Lack of Antiinflammatory Effect. *Arthritis Rheum.* **1972**, *15* (6), 641−643.
(34) Bussotti, L.; D'Auria, M.; Foggi, P.; Lesma, G.; Righini, R.; Silvani, A. The Photochemical Behavior of Colchicone and Thiocolchicone. *Photochem. Photobiol.* **2000**, *71* (1), 29.
(35) Singh, S. P.; Stenberg, V. I.; Parmar, S. S. Photochemistry of Alkaloids. *Chem. Rev.* **1980**, *80* (3), 269−282.
(36) Cacelli, I.; D'Auria, M.; Villani, V. Why Thiocolchicine Does Not Undergo Photochemical Isomerization: A Theoretical Study. *Chem. Phys. Lett.* **2008**, *459* (1−6), 167−171.
(37) Forbes, E. J. Colchicine and Related Compounds. Part XIV. Structure of β- and γ-Lumicolchicine. *J. Chem. Soc.* **1955**, *0* (0), 3864−3870.
(38) Yuan, H.; Guo, X.; Zhang, J. Ab Initio Insights into the Mechanism of Excited-State Intramolecular Proton Transfer Triggered by the Second Excited Singlet State of a Fluorescent Dye: An Anti-Kasha Behavior. *Mater. Chem. Front.* **2019**, *3* (6), 1225−1230.
(39) Ignasiak, M. T.; Houée-Levin, C.; Kciuk, G.; Marciniak, B.; Pedzinski, T. A Reevaluation of the Photolytic Properties of 2-Hydroxybenzophenone-Based UV Sunscreens: Are Chemical Sunscreens Inoffensive? *ChemPhysChem* **2015**, *16* (3), 628−633.
(40) Han, K.; Zhao, G.; Pradhan, R.; Lourderaj, U. Computational Studies on the Excited-State Intramolecular Proton Transfer in Five-Membered-Ring Hydrogen-Bonded Systems. In *Hydrogen-Bonding Research in Photochemistry, Photobiology, and Optoelectronic Materials*; World Scientific, 2019; pp 155−178. DOI: 10.1142/9781786346087_0007.
(41) Majcher, U.; Klejborowska, G.; Moshari, M.; Maj, E.; Wietrzyk, J.; Bartl, F.; Tuszynski, J. A.; Huczyński, A. Antiproliferative Activity and Molecular Docking of Novel Double-Modified Colchicine Derivatives. *Cells* **2018**, *7* (11), 192.
(42) Kerkes, P.; Sharma, P. N.; Brossi, A.; Chignell, C. F.; Quinn, F. R. Synthesis and Biological Effects of Novel Thiocolchicines. 3. Evaluation of N-Acyldeacetylthiocolchicines, N-(Alkoxycarbonyl)-Deacetylthiocolchicines, and O-Ethyldemethylthiocolchicines. New Synthesis of Thiodemecolcine and Antileukemic Effects of 2-Demeth. *J. Med. Chem.* **1985**, *28* (9), 1204−1208.

https://dx.doi.org/10.1021/acs.joc.0c02507
J. Org. Chem. 2021, 86, 11029−11039